



Research Paper

New insights into the biomineralization of mercury selenide nanoparticles through stable isotope analysis in giant petrel tissues

Silvia Queipo-Abad^a, Zoyne Pedrero^{a,*}, Claudia Marchán-Moreno^a, Khoulood El Hanafi^a, Sylvain Bérail^a, Warren T. Corns^b, Yves Cherel^c, Paco Bustamante^{d,e}, David Amouroux^a

^a Université de Pau et des Pays de l'Adour, E2S UPPA, CNRS, IPREM, Institut des Sciences Analytiques et de Physico-chimie pour l'Environnement et les matériaux, Pau, France

^b PS Analytical, Arthur House, Crayfields Industrial Estate, Main Road, Orpington, Kent BR5 3HP, UK

^c Centre d'Etudes Biologiques de Chizé, UMR 7372 CNRS - La Rochelle Université, 79360 Villiers-en-Bois, France

^d Littoral Environnement et Sociétés (LIENSs), UMR 7266 CNRS - La Rochelle Université, 2 rue Olympe de Gouges, 17000 La Rochelle, France

^e Institut Universitaire de France (IUF), 1 Rue Descartes, 75005 Paris, France



ARTICLE INFO

Editor: Dr. R. Deborá

Keywords:

Mercury

Seabirds

Isotopic fractionation

HgSe nanoparticles

MeHg demethylation

ABSTRACT

Tiemanite (HgSe) is considered the end-product of methylmercury (MeHg) demethylation in vertebrates. The biomineralization of HgSe nanoparticles (NPs) is understood to be an efficient MeHg detoxification mechanism; however, the process has not yet been fully elucidated. In order to contribute to the understanding of complex Hg metabolism and HgSe NPs formation, the Hg isotopic signatures of 40 samples of 11 giant petrels were measured. This seabird species is one of the largest avian scavengers in the Southern Ocean, highly exposed to MeHg through their diet, reaching Hg concentrations in the liver up to more than 900 $\mu\text{g g}^{-1}$. This work constitutes the first species-specific isotopic measurement ($\delta^{202}\text{Hg}$, $\Delta^{199}\text{Hg}$) of HgSe NPs in seabirds and the largest characterization of this compound in biota. Similar $\delta^{202}\text{Hg}$ values specifically associated to HgSe ($\delta^{202}\text{Hg}_{\text{HgSe}}$) and tissues ($\delta^{202}\text{Hg}_{\text{bulk}}$) dominated by inorganic Hg species were found, suggesting that no isotopic fractionation is induced during the biomineralization step from the precursor (demethylated) species. In contrast, the largest variations between $\delta^{202}\text{Hg}_{\text{bulk}}$ and $\delta^{202}\text{Hg}_{\text{HgSe}}$ were observed in muscle and brain tissues. This could be attributed to the higher fraction of Hg present as MeHg in these tissues. Hg-biomolecules screening highlights the importance of the isotopic characterization of these (unknown) complexes.

1. Introduction

Mercury (Hg) is a globally distributed pollutant present in polar and sub-polar areas through long-range atmospheric transport (Fitzgerald et al., 1998). Once in the marine environment, inorganic mercury (iHg) can be methylated by microbial activity to form methylmercury (MeHg) (Fitzgerald et al., 2007; Kaschak et al., 2013; Mason, 2013). MeHg bioaccumulates in the tissues of aquatic organisms, and biomagnifies through the food webs resulting in predators at the top of the trophic chain to accumulate large amounts of Hg in their tissues (Mason et al., 1995).

Seabirds in the Southern Hemisphere showed specific patterns of accumulation, distribution and biotransformation of Hg (Albert et al., 2019; Mills et al., 2020; Renedo et al., 2021). Giant petrels are among the top scavengers of these latitudes, feeding on high trophic level

species, which leads to very high concentrations of Hg in their tissues (Renedo et al., 2021). Their great longevity, of up to 50 years old (Foote et al., 2011), coupled with their high trophic position makes them a species of great ecotoxicological interest, as they can bioaccumulate large quantities of toxic elements, especially Hg, which is ingested through the diet as MeHg. Hepatic demethylation is considered a key detoxification pathway of MeHg in seabirds (Kim et al., 1996; Thompson and Furness, 1989) together with its excretion in feathers (Albert et al., 2019). Demethylation involves selenium (Se) (Khan and Wang, 2010), an essential element which presents a high affinity to inorganic mercury (iHg), resulting ultimately in the formation of insoluble tiemanite nanoparticles (HgSe NPs). Although the liver is the key organ for Hg bioaccumulation, HgSe NPs have been found in other organs and tissues of fish, marine mammals and seabirds, including kidneys, muscle and brain (Gajdosechova et al., 2016; Manceau et al., 2021a, 2021b, 2021c).

* Corresponding author.

E-mail address: zoyne.pedrerozayas@univ-pau.fr (Z. Pedrero).

<https://doi.org/10.1016/j.jhazmat.2021.127922>

Received 3 September 2021; Received in revised form 18 November 2021; Accepted 24 November 2021

Available online 27 November 2021

0304-3894/© 2021 Elsevier B.V. All rights reserved.

Hg isotopic analysis in biological samples is a powerful tool to trace Hg trophic sources and metabolic pathways in wildlife (Bolea-Fernandez et al., 2019; Feng et al., 2015; Li et al., 2020; Masbou et al., 2018; Perrot et al., 2016) and in humans (Du et al., 2018; Sherman et al., 2015, 2013). Most of these studies have been carried out on mammalian or fish tissues (Bolea-Fernandez et al., 2019; Feng et al., 2015; Le Croizier et al., 2020; Masbou et al., 2018) and only a few of these studies have focused on seabirds (Manceau et al., 2021b; Poulin et al., 2021; Renedo et al., 2021, 2020, 2018a, 2017). Hg stable isotopes can undergo both mass-dependent fractionation (MDF) and mass-independent fractionation (MIF). Odd Hg isotope MIF is related to the processes of photo-reduction and photodemethylation of Hg mainly in the photic zone, thus allowing traceable marine food source to prey-predator relationships (Kwon et al., 2013; Le Croizier et al., 2020; Renedo et al., 2018b; Sherman et al., 2013). In contrast, the metabolic distribution of Hg in the body can be traced through MDF (Bolea-Fernandez et al., 2019; Feng et al., 2015). This powerful tool has been successfully exploited to track Hg distribution in the tissues of three different seabirds species, revealing that hepatic MeHg demethylation is followed by internal tissue redistribution of the residual MeHg enriched in heavier Hg isotopes (Renedo et al., 2021).

The main aim of this study was to provide new insights into the biomineralization of MeHg into HgSe NPs by the specific isotopic characterization of this inert Hg compound. For this purpose, a large set of giant petrel samples (for a total of 40 tissues) corresponding to 11 individuals of different ages were studied. Complementary analytical techniques have been combined, such as Hg speciation at the chemical and molecular level, as well as Hg and Se measurements between solid and soluble fractions of tissues. The current work represents the first study on Hg isotopic characterization specifically associated to NPs in (sea)birds. Hg isotopic analyses in blood, as well as the comparison between Hg isotopic composition in HgSe NPs and bulk tissues, shedding light about different distribution routes between tissues of seabirds.

2. Material and methods

2.1. Ecological characteristics of giant petrels

The avian model corresponds to the two sibling species of giant petrels, the northern (*Macronectes halli*) and southern (*Macronectes giganteus*) giant petrels, which are the dominant scavengers of the Southern Ocean (Rheinhardt and Austin, 2005; Salomon and Voisin, 2010). Giant petrels are large birds that can reach over two meters of wingspan (Carlos and Voisin, 2008). During the reproduction period, adult males feed mostly on land on carrion, seabirds and pinnipeds, while females mainly forage at sea, preying on fish, squid and krill (Thiers et al., 2014).

2.2. Sampling set and individual characteristics

Eleven dead individuals of giant petrels were opportunistically collected. Four of them were *M. halli* (all males) and were collected in the Kerguelen archipelago (Southern Indian Ocean) in 2014. The other four birds were *M. giganteus*. One specimen was collected in the Kerguelen Archipelago in 2014 (male) and three were collected in Adélie Land (Antarctic continent) in 2019 (1 female and 2 males). The age of these individuals could not be precisely determined, but one of the seabirds collected in Adélie Land was a fully-fledged chick (viz. less than 1 year old). In addition to this, samples of three other adults *M. giganteus* (see details in Renedo et al., 2021) from the same region were also considered in the present study. The samples from Adélie Land were in good shape for adults who died after a collision against an electric pole, but the chick (P-P1) was very emaciated suggesting it dies from starvation. For all the others, the cause of death is unknown. All of them were collected freshly after their death. Internal tissues were sampled, weighed, and stored individually in plastic bags. Liver, kidneys and pectoral muscle were collected from all the eight birds, while brain

tissue was sampled for the three *M. giganteus* collected in 2019. Blood samples were obtained by collecting clotted blood from heart atria. After dissection, all the samples were stored at $-20\text{ }^{\circ}\text{C}$. All details relating to the complete sampling set are provided in Table S1. All the tissues used in this work were homogenized with an ultra-turrax® and a portion was freeze-dried for analytical purposes.

2.3. Determination of total Hg, Se and Hg species

2.3.1. Determination of Hg and Se concentrations

Freeze-dried and homogenized tissue samples (0.05–0.10 g) were digested in 3 mL of Trace Metal Grade HNO_3 (Fisher scientific, Illkirch, France) in an Ultrawave microwave digestion system (Milestone, Sorisole, Italy) at $220\text{ }^{\circ}\text{C}$ for 10 min. Fresh-frozen blood samples were digested directly without freeze-drying. The measurement of total Hg (THg) in the digests was performed by cold vapor – atomic fluorescence spectrometry (CV-AFS PS Analytical 10.025, Kent, UK) by reduction with 3% (m/v) SnCl_2 (Scharlab, Barcelona, Spain) in 10% (v/v) HCl (J.T. Baker, Fisher scientific, Illkirch, France). The samples were then diluted in HCl 5% (v/v) for analyzes and the quantification was performed by standard calibration. For Se analyses, the resulting digests were appropriately diluted with Milli-Q water and analyzed by ICP-MS. Method protocols were validated using certified reference materials (BCR-464, NIST-1947 and DOLT-5). The information relative to the quality assurance of the analyses of Hg and Se is found in Table S2.

2.3.2. Determination of iHg and MeHg species

Between 0.05 and 0.10 g of freeze-dried samples was added to glass vessels together with 3 mL of 25% (m/v) tetramethylammonium hydroxide (TMAH) and a magnetic stir bar. For blood, Hg species were directly extracted from the freshly frozen samples. Vials were closed with a Teflon cap and placed in the microwave. The focused microwave assisted extraction of the samples was performed using a Discover SP-Microwave (CEM Corporation, Matthews, NC). The extraction was carried out using a 1-min ramp up to $75\text{ }^{\circ}\text{C}$ followed by 3 min at $75\text{ }^{\circ}\text{C}$ with constant stirring. Inorganic mercury (iHg) was measured by CV-AFS after dilution of the extract in HCl 5% (v/v) (Davis et al., 2007; Davis and Long, 2011; Renedo et al., 2021). For the determination of total Hg, 50 μL of a 0.1 N (0.05 mol/L cBr_2) potassium bromide/bromate solution (Merck, Darmstadt, Germany) was added to 10 mL of the diluted digest in 5% (v/v) HCl. The CV-AFS system was coupled to an oxidation unit (PS Analytical 10.820, Kent, UK) equipped with a UV lamp so that all samples with potassium bromide/bromate were subjected to on-line UV irradiation to facilitate immediate oxidation of MeHg and subsequent measurement of THg. The concentration of MeHg was determined by the subtraction of iHg from the THg concentration (Aranda et al., 2009; Kaercher et al., 2005). This procedure was validated using BCR-464 and TORT-2 as shown in Table S2.

2.4. Determination of Hg biomolecular species by SEC-ICP-MS

The aqueous soluble protein fraction was extracted from fresh samples (approximately 0.1 g) by ultra-probe sonication (30 s at 100 W power) in 3 mL of 100 mM ammonium acetate (pH 7.4) followed by centrifugation, as described elsewhere (Pedrero et al., 2011). The obtained cytosolic biomolecules were separated by size exclusion chromatography (SEC) using a Superdex 200 300/10 column (10 mm ID \times 300 mm length \times 13 μm particle size) (GE Healthcare, Uppsala, Sweden). A HPLC Agilent 1100 (Agilent, Wilmington, DE) equipped with a binary HPLC pump and an autosampler was coupled to an Agilent ICP-MS 7500ce (Yokogawa Analytical Systems, Tokyo, Japan). The supernatant was analyzed by injection of 100 μL fractions. Isocratic elution was performed at 0.7 mL min^{-1} with a mobile phase of 100 mM ammonium acetate at pH of 7.4 (Pedrero et al., 2011; Pedrero Zayas et al., 2014).

2.5. Extraction of HgSe nanoparticles

Isolation of HgSe NPs was carried out by using an adaptation of the method described elsewhere (Bolea-Fernandez et al., 2019; Gajdosechova et al., 2016). In brief, after defatting, a soft acid treatment with formic acid was applied to the samples. The resulting extract was centrifuged by using 50 kDa cut-off filters (Amicon Ultra). The filter was abundantly washed with Milli-Q water until total removal of soluble Hg and Se was achieved (Gajdosechova et al., 2016). Nanoparticles were then recovered by centrifugation for 3 min at $1000 \times g$. The collected NPs were then digested in 3 mL HNO_3 , using the procedure described in Section 2.3. This selective extraction protocol is not considered to be quantitative, due to losses in the cut-off filtration steps. The procedure however has been successfully used for Hg isotopic characterization previously since no isotopic fractionation of this solid species is induced during the sample treatment (Bolea-Fernandez et al., 2019).

2.6. Hg stable isotope analysis

Hg isotopic ratios were measured using a multicollector-(MC)-ICP-MS (Nu Instruments, Wrexham, UK) coupled with continuous flow cold vapor generation (CVG) on the digested samples (see above). The isotopes ^{198}Hg , ^{199}Hg , ^{200}Hg , ^{201}Hg , ^{202}Hg , ^{203}Tl , ^{204}Hg , and ^{205}Tl were simultaneously measured in the Faraday cups L2, L1, Ax, H1, H2, H3, H4 and H5, respectively. In order to correct the instrumental mass-bias, NIST SRM 997 thallium standard solution in 2% (v/v) of HNO_3 (Optima grade, Fisher scientific, Illkirch, France) was nebulized continuously through a desolvation unit (DSN) and the calculation was performed using the exponential law model (Bergquist and Blum, 2007; Blum and Bergquist, 2007; Perrot et al., 2010). The sample standard bracketing (SSB) approach was employed for the calculation of isotope ratios relative to the NIST 3133-iHg standard solution. Mass dependent fractionation (MDF) is reported as recommended by Bergquist and Blum (2007) relative to the NIST 3133 Hg solution using Eq. (1):

$$\delta^{xxx}\text{Hg} = \left(\frac{{}^{xxx/198}\text{Hg}_{\text{sample}}}{{}^{xxx/198}\text{Hg}_{\text{NIST 3133}}} - 1 \right) * 1000 \quad \text{‰} \quad (1)$$

where xxx is the studied isotope. Mass-independent fractionation (MIF) of Hg is reported using Eq. (2) as the difference between the theoretical value predicted by MDF and the measured values as $\Delta^{199}\text{Hg}$ and $\Delta^{201}\text{Hg}$ in ‰, according to the protocol suggested elsewhere (Blum and Bergquist, 2007):

$$\Delta v_{xxx}\text{Hg} = \delta^{xxx}\text{Hg} - (\delta^{202}\text{Hg} \times \beta_{xxx}) \quad (2)$$

where β_{xxx} is the kinetic mass-dependence scale factor that depends on the isotopes (0.2520 for ^{199}Hg , 0.5024 for ^{200}Hg , 0.7520 for ^{201}Hg and 1.493 for ^{204}Hg) (Blum and Bergquist, 2007). All the samples and standards were measured at a concentration of 1 ng g^{-1} of Hg in a 10% (v/v) HNO_3 /2% (v/v) HCl solution, to avoid any bias caused by differences in concentration. The external reproducibility of the measurements is expressed as $\pm 2\text{SD}$ for 35 measurements of the NIST RM 8610 (former UM Almadén) as 0.09 and 0.05 ‰ for $\delta^{202}\text{Hg}$ and $\Delta^{199}\text{Hg}$, respectively. All the values for the isotopic composition of the NIST RM 8610 and the certified reference materials BCR-464, NIST 1947 and TORT-2 analyzed in this work are presented in Table S3.

3. Results and discussion

3.1. Hg concentrations in giant petrel tissues

The total mercury (THg) concentrations in the tissues of giant petrels are among the highest ever reported for seabirds, up to $933 \mu\text{g g}^{-1}$ dry weight (d.w. here and in all reported concentration values) (Table S4). However, THg was highly variable among tissues for each individual

and among individuals considering a single tissue. Nonetheless, the liver always showed the highest concentrations among tissues with Hg hepatic concentrations ranging from 99 to $933 \mu\text{g g}^{-1}$ (mean value of 419 ± 317 , $n = 9$) for adult giant petrels. These values are in agreement with previously reported values for giant petrels from New Zealand (Stewart et al., 1999). As liver is the main storage organ for Hg in vertebrates, hepatic concentrations provide an indirect indication of the age of animals (Bolea-Fernandez et al., 2019; Gajdosechova et al., 2016). Thus, our sampling covers a large range of ages allowing us to consider if this factor influences the detoxification process of MeHg. The only chick of the study (P-P1) presents the lowest Hg levels in all the tissue types. The Hg concentration in liver of the chick individual ($1.1 \mu\text{g g}^{-1}$) is consistent by the process of bioaccumulation with age. In kidneys, THg concentrations were higher for most of the adult samples ranging from 7.8 to $481 \mu\text{g g}^{-1}$ (mean value of 85 ± 140 , $n = 10$) than the already previously reported concentrations for petrels and other large seabirds such as albatrosses (Bocher et al., 2003; Cipro et al., 2014; Kim et al., 1996; Stewart et al., 1999). In muscles, Hg concentrations vary from 1.0 to $52 \mu\text{g g}^{-1}$ (mean value of 18 ± 20 , $n = 9$) in adults ($0.10 \mu\text{g g}^{-1}$ for the chick), and are among the highest reported for seabirds (Renedo et al., 2021). In the case of blood, the two adults from the Antarctic continent (P-10, P-11) exhibit concentrations around $0.5 \mu\text{g g}^{-1}$ (wet weight), which was fivefold higher than the concentration found in the chick (P-P1) from the same location. A linear correlation (Pearson's correlation coefficient $\rho = 0.8971$) was found between THg concentrations in liver and muscle (Fig. S1), which could indicate that Hg bioaccumulation occurs in both tissues along time, Hg being mainly retained in the liver but its excess being directly transferred towards the muscles as suggested by previous studies (Manceau et al., 2021; Renedo et al., 2021).

Despite the high variability of MeHg content among individuals (Table S4), likely due to their age difference (Gajdosechova et al., 2016), the percentage of organic Hg was higher in brain (34–74%) than in liver and kidneys (2–34%). Regarding muscles, in the adults with lower Hg concentrations (P-10 and P-11, both from the Antarctic continent), the MeHg fraction reaches up to 71%. In contrast, in the case of individuals showing higher liver THg concentrations, the percentage of MeHg in the muscles was much lower (8–30%), suggesting that the proportion of MeHg decreases with age together with an increase of THg concentrations. Such a trend was already reported for top of the marine food chain marine mammals including seals and toothed whales (Bolea-Fernandez et al., 2019; Dehn et al., 2005; Gajdosechova et al., 2016).

4. Hg isotopic composition of tissues: understanding Hg (re) distribution

The high $\delta^{202}\text{Hg}_{\text{bulk}}$ variability in the different tissues analyzed contrasts with the quite homogenous $\Delta^{199}\text{Hg}_{\text{bulk}}$ values obtained whatever the tissue (Table S5). Thus, MIF ($\Delta^{199}\text{Hg}_{\text{bulk}}$) ranges from 1.13 ‰ to 1.73 ‰ among individuals, except in the case of the chick, which present the lowest values of the study. Considering the whole data set, the $\Delta^{199}\text{Hg}/\Delta^{201}\text{Hg}$ slope is 1.13 ± 0.01 ($r = 0.968$), similar to slope values reported for other marine top predators and fish (Fig. S2) (Le Croizier et al., 2020; Masbou et al., 2018; Renedo et al., 2018, 2021). The reference $\Delta^{199}\text{Hg}/\Delta^{201}\text{Hg}$ slopes for MeHg photodemethylation processes (1.36 ± 0.02) and iHg photoreduction (1.00 ± 0.02) (Bergquist and Blum, 2007) are also presented in Fig. S2. The values of $\Delta^{199}\text{Hg}$ for giant petrel tissues agree with those of blood in skua chicks (1.14 ± 0.05 ‰) and subantarctic penguins (1.16 ± 0.05 ‰), which were correlated with latitude (Renedo et al., 2020). Interestingly, MIF values in the single chick collected on the Antarctic continent (P-P1) ranged from 0.88 ‰ to 1.1 ‰ for internal tissues, being slightly lower than for the adults. Giant petrel chicks are fed with prey caught near the colony by their parents. Hence, the MIF difference is likely due to its exclusively Antarctic food sources that are characterized by low $\Delta^{199}\text{Hg}$ values (Renedo et al., 2020). In contrast, adults sampled in the Antarctic

Continent may reflect an integration of Hg from local prey during the breeding season and Hg prey from lower latitude during the wintering season (Renedo et al., 2021).

MDF ($\delta^{202}\text{Hg}_{\text{bulk}}$) values ranged widely from -1.48‰ up to 3.05‰ (Table S5). In all the individuals, the highest $\delta^{202}\text{Hg}$ values correspond to blood samples. The specific differences of $\delta^{202}\text{Hg}$ values between tissues (Fig. 1) is attributed to the strong dependence on the ratio of methylated and demethylated Hg (Feng et al., 2015; Perrot et al., 2016; Renedo et al., 2021). MeHg demethylation induces mass dependent fractionation, resulting in an enrichment of the inorganic Hg species in lighter isotopes whilst the residual MeHg is enriched in heavier ones (Perrot et al., 2016; Rodríguez-González et al., 2009). The highest MDF values in blood, also observed in other animal studies, is understood as a consequence of the transport of residual MeHg (enriched in heavier isotopes from incomplete demethylation processes) by the blood stream (Bolea-Fernandez et al., 2019; Li et al., 2020; Ma et al., 2018; Renedo et al., 2021)

Regarding brain, it is generally enriched in heavier isotopes ($\delta^{202}\text{Hg}$ 0.03–1.77 ‰) in comparison to liver and kidneys (Table S5), suggesting residual MeHg from the blood streams subsequently accumulate in this organ. In the case of muscles, two different trends are identified (Fig. 1, Table S5) according to the hepatic Hg concentration (associated to the age of the animals). Muscles of giant petrel individuals with the highest THg hepatic concentrations ($250\text{--}933\text{ }\mu\text{g g}^{-1}$) are enriched in lighter isotopes ($\delta^{202}\text{Hg}$) in comparison to liver and kidneys, contrasting with muscles of the other group of animals (THg hepatic concentrations lower than $250\text{ }\mu\text{g g}^{-1}$). Even though Hg isotopic characterization in animal's internal tissues is not extensive, the trend observed in the mentioned samples is in agreement with previous studies on marine mammals and seabirds (Bolea-Fernandez et al., 2019; Li et al., 2020; Renedo et al., 2021) and is attributed to the higher proportion of MeHg in muscles than in the liver. As previously discussed, this organomercurial species is expected to be enriched in heavier isotopes compared to the demethylated ones, assuming preferential demethylation of the lighter Hg isotopes (Perrot et al., 2016; Rodríguez-González et al., 2009).

Noticeably, the giant petrel individuals with the highest THg hepatic concentrations (oldest ones) exhibit lighter $\delta^{202}\text{Hg}$ ($\delta^{202}\text{Hg}_{\text{bulk}}$) values in muscles than in liver and kidneys (Tables S4 and S5). Similarly, a recent investigation in marine mammals reported a decrease of $\delta^{202}\text{Hg}$ values in the muscles of the individuals from the oldest group in comparison to the juvenile one (a shift of 0.8‰ between both groups) (Bolea-Fernandez et al., 2019). Atypically, muscles of those giant petrels

contained mainly iHg (70–93%). This particular enrichment of muscles in demethylated Hg species is the most likely reason why muscles of these old seabirds contain lighter Hg isotopes, highlighting that demethylation occurs effectively in this tissue as previously reported (Manceau et al., 2021c). Furthermore, several pathways and factors could also influence the stable isotope signature. One of them is the MeHg excretion by molting, a well-known excretion strategy in birds (Bearhop et al., 2000) when MeHg is massively remobilized from internal tissues towards the growing feathers (Renedo et al., 2021). Thus, between 70% and 90% of the Hg load of the birds is excreted into the new plumage during molting (Agusa et al., 2005; Braune and Gaskin, 1987). In addition, the ageing process intensely impacts, among others, muscle metabolism (Burger, 1993; Wone et al., 2018) and could result in MeHg mobilization (Cuvin-Aralar and Furness, 1991). Moreover, specifically in migrating birds, the consumption of energy stores during migratory fasting could contribute to MeHg mobilization and higher MeHg circulating levels (Seewagen et al., 2016). Therefore, the atypical muscle Hg speciation and isotopic composition in the oldest giant petrels could be the result of the different mechanisms mentioned above.

4.1. Hg isotopic composition of HgSe nanoparticles (tiemannite)

The present work is the first to isolate and measure the Hg isotopic composition of HgSe NPs in seabird tissues. The specific Hg isotopic composition associated to HgSe NPs ($\delta^{202}\text{Hg}_{\text{HgSe}}$) was compared with the bulk ($\delta^{202}\text{Hg}_{\text{bulk}}$) value (Fig. 2, Table S5). In general, in individuals exhibiting the highest THg hepatic concentrations ($250\text{--}933\text{ }\mu\text{g g}^{-1}$), a match for both MDF and MIF, was observed in liver and kidneys between THg ($\delta^{202}\text{Hg}_{\text{bulk}}$) and HgSe NPs ($\delta^{202}\text{Hg}_{\text{HgSe}}$) (typically represented in Fig. 2. A for seabird P-1). The specific isotopic signature in isolated HgSe NPs found in the muscles of this set of individuals was also quite similar to the isotopic values in the whole tissue. In the other set of individuals (THg hepatic concentrations lower than $250\text{ }\mu\text{g g}^{-1}$), the $\delta^{202}\text{Hg}$ difference between THg and HgSe NPs showed dissimilar trends depending on tissues. Contrary to muscles and brain, most of HgSe NPs in kidneys are enriched in heavier isotopes ($\delta^{202}\text{Hg}$ shift up to 0.56‰) in comparison to the bulk (Fig. 2.D, Table S5) while no tendency is identified in the liver of these individuals. The mentioned pattern, specifically observed in kidneys, could be related to a physiological peculiarity in birds, where a renal portal system allows this organ to be bypassed (Meredith and Johnson-Delaney, 2010). Considering that HgSe NPs is the final product of MeHg breakdown, the observed ^{202}Hg -enrichment of this solid species in liver and kidneys is unexpected. The previous report of Hg isotopic characterization in HgSe is limited to long-finned pilot whales (five livers and two muscles) (Bolea-Fernandez et al., 2019). It is therefore interesting to note a total agreement in the obtained trends in livers and muscles of both animals belonging to two classes of vertebrates.

In the giant petrel group exhibiting the highest Hg hepatic concentrations, there is a perfect match between the isotopic signature of THg ($\delta^{202}\text{Hg}_{\text{bulk}}$) and those in HgSe NPs ($\delta^{202}\text{Hg}_{\text{HgSe}}$) for the liver, kidneys and muscles. In those samples, iHg species were the dominant ones (Table S4), with HgSe constituting 95 ± 5 , 61 ± 8 and $35 \pm 15\%$ in liver, kidneys, and muscle, respectively according to X-ray absorption near edge structure (XANES) analyses (Manceau et al., 2021c). In addition to HgSe NPs, another iHg complex exhibiting a molar ratio Hg:Se (1:4) has been reported by these authors. This complex was described as mercury selenocysteinate, $\text{Hg}(\text{SeCys})_4$ which is considered to be precursor of tiemannite. $\text{Hg}(\text{SeCys})_4$ was found to be present in liver, kidneys, and muscles representing 5 ± 2 , 35 ± 10 and $61 \pm 13\%$ of the THg, respectively (Manceau et al., 2021c). In each tissue, the THg isotopic composition results from the contribution of different Hg species as outlined in Eq. (3):

$$\delta^{202}\text{Hg}_{\text{bulk}} = f_{\text{MeHg-R}} \times \delta^{202}\text{Hg}_{\text{MeHg-R}} + f_{\text{iHg}} \times \delta^{202}\text{Hg}_{\text{iHg}} \quad (3)$$

where f is the fraction of each species in the bulk tissue and the

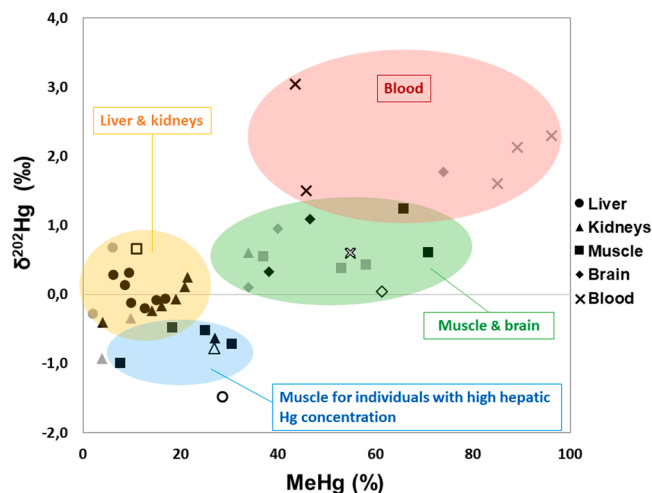


Fig. 1. $\delta^{202}\text{Hg}$ plotted against the percentage of MeHg for the 41 tissue samples of giant petrels. Grey markers correspond to isotopic values reported elsewhere (Renedo et al., 2021) in a pilot study for three giant petrels (PGA01, PGA02 and PGA03). White-filled markers correspond to isotopic values of the youngest individual (P-P1).

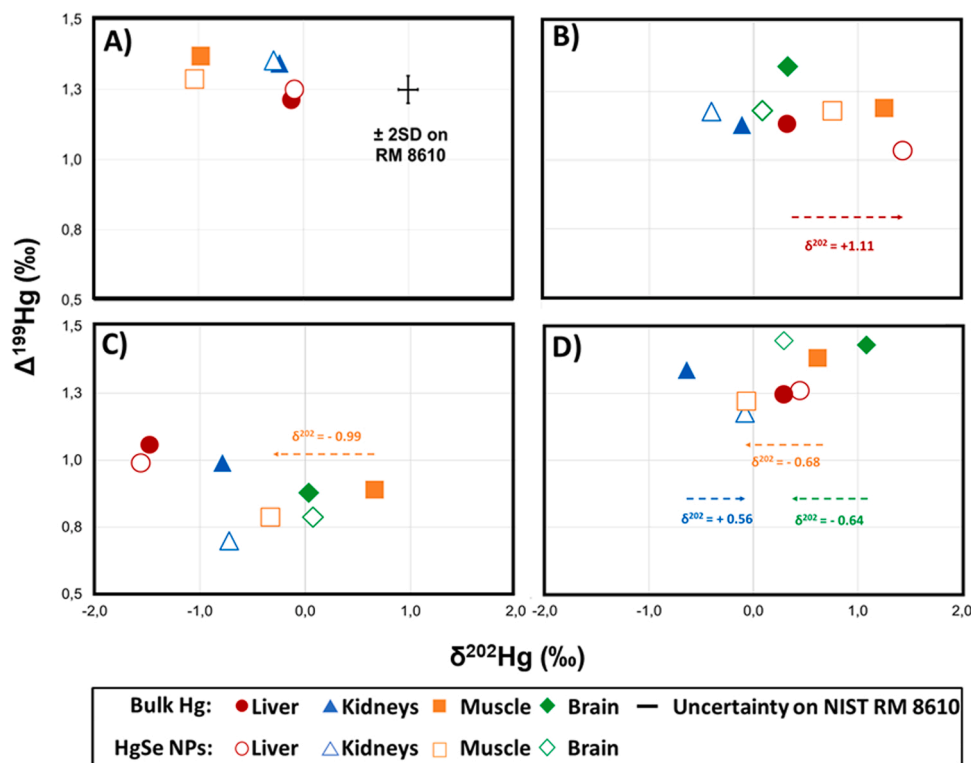


Fig. 2. $\Delta^{199}\text{Hg}$ vs $\delta^{202}\text{Hg}$ values for liver, kidneys and muscle of giant petrels: A) P-1, B) P-11, C) P-P1 and D) P-10. Dotted arrows correspond to the shift between $\delta^{202}\text{Hg}$ values from THg to HgSe NPs in different organs. Uncertainties in the measurement of the isotopic ratios are expressed as 2SD on the secondary standard RM 8610.

contribution of the iHg species could be expressed as follows in Eq. (4):

$$\delta^{202}\text{Hg}_{\text{iHg}} = f_{\text{HgSe}} \times \delta^{202}\text{Hg}_{\text{HgSe}} + f_{\text{Hg:Se}(1:4)} \times \delta^{202}\text{Hg}_{\text{Hg:Se}(1:4)} \quad (4)$$

In the described set of samples with the highest Hg concentrations in the liver, the $\delta^{202}\text{Hg}_{\text{bulk}}$ and $\delta^{202}\text{Hg}_{\text{HgSe}}$ are identical (Table S5) irrespectively of the proportion of both inorganic species (HgSe and $\text{Hg}(\text{SeCys})_4$). Therefore, we propose that the mentioned inorganic species share a similar $\delta^{202}\text{Hg}$ signature. This finding suggests that no isotopic fractionation seems to be induced during the biomineralization (HgSe NPs) step from the precursor species Hg:Se (1:4).

On the other hand, the largest shifts between $\delta^{202}\text{Hg}$ in bulk and the one specifically associated to HgSe NPs are found in muscles and brain (Table S5). The observed variations could be attributed to the higher fraction of Hg present as MeHg in these two tissues. The organomercurial compound is expected to be specifically enriched in heavier isotopes, since MeHg demethylation is followed by internal tissue redistribution of the residual MeHg enriched in heavier Hg isotopes (Bolea-Fernandez et al., 2019; Li et al., 2020; Ma et al., 2018; Renedo et al., 2021).

The brain was the organ exhibiting the highest MeHg percentage (Table S4), where HgSe and Hg:Se (1:4) have been also reported (Manceau et al., 2021c). The specific isotopic signature of the organic compound ($\delta^{202}\text{Hg}_{\text{MeHg}}$) could be estimated by considering: *i.* the proportion of these inorganic species (Table S4 and XANES data) and *ii.* assuming HgSe and Hg:Se (1:4) share a similar MDF pattern ($\delta^{202}\text{Hg}_{\text{HgSe}}$ in Table S5). The obtained $\delta^{202}\text{Hg}_{\text{MeHg}}$ values vary between 1.98 ‰ and 2.94 ‰ for the investigated individuals, confirming an enrichment in lighter isotopes of the demethylated iHg with respect to MeHg (Fig. 3). The isotopic measurement in each individual species is undoubtedly the best approach to determine the species-specific isotopic signature. The obtained (estimated) values are in good agreement with the shift ($\sim 3\%$ $\delta^{202}\text{Hg}$) between MeHg and iHg species measured by Gas Chromatography coupled to MC-ICPMS, the single study so far that has measured

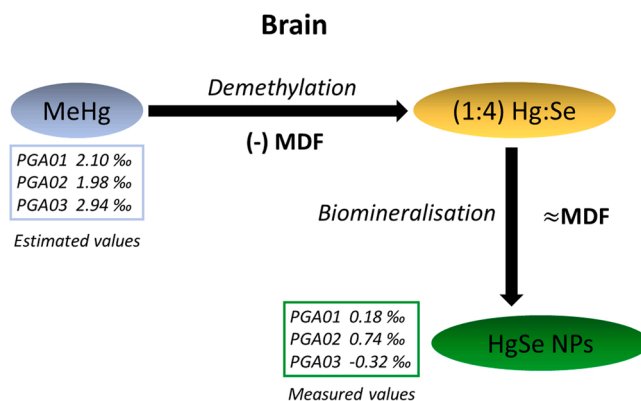


Fig. 3. Simplified diagram for the estimation of MDF ($\delta^{202}\text{Hg}$) values of MeHg according to the new insights found for the demethylation/biomineralization of MeHg into HgSe NPs in brain of three giant petrels (PGA01, PGA02 and PGA03).

both Hg species in animals (Perrot et al., 2016).

Chemical speciation and (total) Hg isotopic analyses have been combined in several recent studies for the estimation of Hg species-specific isotopic signature (Feng et al., 2015; Li et al., 2020; Poulin et al., 2021). The mentioned approach has provided new and valuable information on Hg in biota, however it should be emphasized that Hg speciation has been simplistically reduced to inorganic and MeHg species, without considering the binding of Hg with biomolecules and proteins (Pedrero et al., 2016).

4.2. New insights on Se-mediated MeHg breakdown

Despite the great interest related to the understanding of MeHg

transformation into the bioinert HgSe NPs (Cid-Barrio et al., 2020), the mechanism is still not fully characterized. According to our results, it seems that the limiting step in the detoxification of MeHg leading to the formation of HgSe NPs is the cleavage of the C-Hg bond. The mentioned MeHg demethylation step is associated with a MDF shift varying between 2 ‰ and 3 ‰ (Fig. 3), in total agreement with species-specific isotopic values reported in the literature (Perrot et al., 2016; Poulin et al., 2021; Rodríguez-González et al., 2009). This route would be mediated by Se-biomolecules (Asaduzzaman and Schreckenbach, 2011; Khan and Wang, 2010), finally leading to HgSe precipitation in the tissues (Palmisano et al., 1995). The hypothesis that this stage is thermodynamically favorable (Banerjee et al., 2015) could explain the absence of measurable isotopic fractionation between the two inorganic species, the (demethylated) Hg intermediate complex and the HgSe NPs. Deeper investigation focused on Se speciation in giant petrel tissues has revealed that selenoneine is the main Se-compound whatever the considered tissue (authors' unpublished data). The potential involvement of selenoneine in Hg detoxification has been evoked in several works (Achouba et al., 2019; Yamashita et al., 2013). One of the most advanced hypothesis is the mediation of selenoneine in the cleavage of Hg–methyl bonds, based on the demonstration of such capability by 1-methyl-1,3-dihydro-2H-benzimidazole-2-selone, H(sebenzimMe) a structural analogue of the selenoneine (Palmer and Parkin, 2015). The resulting MeHg demethylation compound presents a molar ratio Hg:Se of 1:4 (Palmer and Parkin, 2015) as the one reported on giant petrel samples (Manceau et al., 2021c).

The complexity of Hg metabolism, including MeHg demethylation, is unquestionable. In general, Hg speciation is mainly limited to the discrimination between inorganic and organic species, with no consideration of Hg linked to proteins and other biomolecules (Pedrero et al., 2016). In the set of samples investigated, a lower Hg proportion was associated to the water-soluble fraction (Table S4). The screening by size exclusion chromatography of the water extractable fraction of internal tissues of giant petrels reveals the presence of several Hg compounds (Fig. 4). The diversity of (unknown) Hg species detected in the water-soluble fraction strongly suggests the complexity of Hg metabolic pathways and its interactions with biomolecules in living organisms. The structural identification of Hg metabolites is limited so far to few examples as hemoglobin (-MeHg) and metallothioneins (-iHg) in marine mammals (Pedrero et al., 2011; Pedrero Zayas et al., 2014), peptide complexes in plants (Krupp et al., 2009) and ethylmercury adduct formation of human serum albumin and β -lactoglobulin (Trümpler et al., 2009) due to the great analytical challenges they represent. Despite the significant advances on the understanding of Hg in biota from this and other recent studies (Bolea-Fernandez et al., 2019; Gajdosechova et al., 2016; Manceau et al., 2021c; Pedrero et al., 2012; Pedrero Zayas et al., 2014; Poulin et al., 2021), species-specific isotopic characterization of Hg compounds, including Hg-biomolecules is mandatory to go further on the characterization of Hg metabolic pathways.

5. Conclusions

In this study, for the first time HgSe NPs species-specific (Hg) isotopic characterization has been carried out in seabirds. The isotopic signature of this compound, which is considered to be the end-product of MeHg demethylation, was determined in numerous tissues including liver, muscle, kidney and brain tissues of individual giant petrels. The Hg isotopic composition matching of HgSe NPs (measured) and other inorganic species (estimated) indicates that no isotopic fractionation appears to be induced during the HgSe NPs biomineralization step from the precursor-demethylated species. The comparison between species-specific Hg isotopic composition of MeHg (estimated) and demethylated species, suggests that a shift of 2–3 ‰ $\delta^{202}\text{Hg}$ could be associated to the cleavage of the C-Hg bond. On the other hand, the screening of water-extractable Hg binding proteins from different tissues reveals the presence of several (unknown) Hg species, probably involved on MeHg

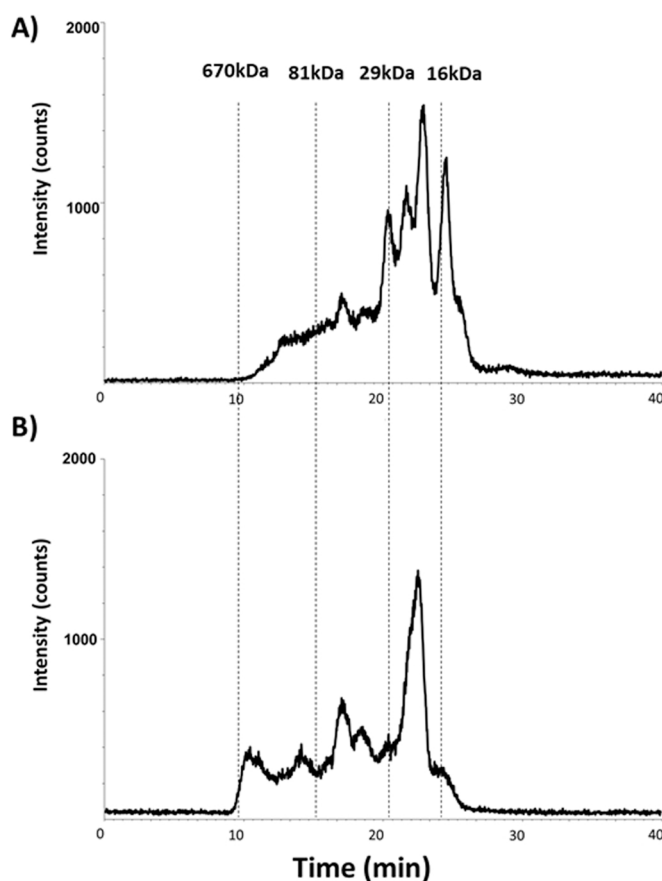


Fig. 4. Typical ^{202}Hg chromatogram obtained by SEC-ICP-MS for the water-soluble fraction of: A) liver and B) kidneys of adult giant petrels.

detoxification. Advances in analytical chemistry allowing isolation and/or characterization by hyphenated techniques (e.g. HPLC-MC-ICPMS) will be crucial to accurately determine the Hg isotopic composition in these species and understand their role on Hg metabolism.

CRediT authorship contribution statement

S.Q.-A.: Conceptualization, Methodology, Writing – original draft, Writing – review & editing. **Z.P.:** Design of the experiment, Conceptualization, Supervision, Validation, Writing – review & editing. **C.M.-M., K.E.H. and S. B.:** Methodology. **W.C.** has provided analytical and technical support, Validation, Writing – review & editing. **Y. C.:** Conceptualization, Validation, Writing – review & editing. **P. B.:** Conceptualization, Validation, Writing – review & editing. **D.A.:** Conceptualization, Supervision, Validation, Writing – review & editing.

Declaration of Competing Interest

The authors declare that they have no known competing financial interests or personal relationships that could have appeared to influence the work reported in this paper.

Acknowledgements

The authors thank the Agence Nationale de la Recherche (MERSEL Project no. ANR-18-CE34-0004-01), CNRS (MITI-ISOISEAUX) and the Communauté d'Agglomération Pau Béarn Pyrénées (MERISOTOP) for their financial support. This project has also received funding from the European Union's Horizon 2020 research and innovation programme under the Marie Skłodowska-Curie Grant Agreement no. 101007962". S.

Queipo and C. Marchan Moreno acknowledge their postdoctoral and Ph.D. fellowships, respectively, funded by the Région Nouvelle Aquitaine (Project BENESEL). Support was provided to Yves Chérel by the Institut Polaire Français Paul Emile Victor (IPEV programme no. 109, C. Barbraud) and the Terres Australes et Antarctiques Françaises, and to Paco Bustamante by the Institut Universitaire de France (IUF). The authors would like to acknowledge PS Analytical for their instrumental and technical support.

Appendix A. Supplementary material

Supplementary data associated with this article can be found in the online version at doi:10.1016/j.jhazmat.2021.127922.

References

- Achouba, A., Dumas, P., Ouellet, N., Little, M., Lemire, M., Ayotte, P., 2019. Selenoneine is a major selenium species in beluga skin and red blood cells of Inuit from Nunavik. *Chemosphere* 229, 549–558. <https://doi.org/10.1016/j.chemosphere.2019.04.191>.
- Agusa, T., Matsumoto, T., Ikemoto, T., Anan, Y., Kubota, R., Yasunaga, G., Kunito, T., Tanabe, S., Ogi, H., Shibata, Y., 2005. Body distribution of trace elements in black-tailed gulls from Rishiri Island, Japan: age-dependent accumulation and transfer to feathers and eggs. *Environ. Toxicol. Chem.* 24, 2107–2120. <https://doi.org/10.1897/04-617R.1>.
- Albert, C., Renedo, M., Bustamante, P., Fort, J., 2019. Using blood and feathers to investigate large-scale Hg contamination in Arctic seabirds: a review. *Environ. Res.* 177, 108588. <https://doi.org/10.1016/j.envres.2019.108588>.
- Aranda, P.R., Pacheco, P.H., Olsina, R.A., Martínez, L.D., Gil, R.A., 2009. Total and inorganic mercury determination in biodiesel by emulsion sample introduction and FI-CV-AFS after multivariate optimization. *J. Anal. At. Spectrom.* 24, 1441–1445. <https://doi.org/10.1039/b903113h>.
- Asaduzzaman, A.M., Schreckenbach, G., 2011. Degradation mechanism of methyl mercury selenoamino acid complexes: a computational study. *Inorg. Chem.* 50, 2366–2372. <https://doi.org/10.1021/ic1021406>.
- Banerjee, M., Karri, R., Rawat, K.S., Muthuvel, K., Pathak, B., Roy, G., 2015. Chemical detoxification of organomercurials. *Angew. Chem.* 127, 9455–9459. <https://doi.org/10.1002/ange.201504413>.
- Bearhop, S., Ruxton, G.D., Furness, R.W., 2000. Dynamics of mercury in blood and feathers of Great Skuas. *Environ. Toxicol. Chem.* 19, 1638–1643. [https://doi.org/10.1897/1551-5028\(2000\)019<1638:DOMIBA>2.3.CO;2](https://doi.org/10.1897/1551-5028(2000)019<1638:DOMIBA>2.3.CO;2).
- Bergquist, B.A., Blum, J.D., 2007. Mass-dependent and -independent fractionation of Hg isotopes by photoreduction in aquatic systems. *Science* 318 (80), 417–420. <https://doi.org/10.1126/science.1148050>.
- Blum, J.D., Bergquist, B.A., 2007. Reporting of variations in the natural isotopic composition of mercury. *Anal. Bioanal. Chem.* 388, 353–359. <https://doi.org/10.1007/s00216-007-1236-9>.
- Bocher, P., Caurant, F., Miramand, P., Chérel, Y., Bustamante, P., 2003. Influence of the diet on the bioaccumulation of heavy metals in zooplankton-eating petrels at Kerguelen archipelago, Southern Indian Ocean. *Polar Biol.* 26, 759–767. <https://doi.org/10.1007/s00300-003-0552-6>.
- Bolea-Fernandez, E., Rua-Ibarz, A., Krupp, E.M., Feldmann, J., Vanhaecke, F., 2019. High-precision isotopic analysis sheds new light on mercury metabolism in long-finned pilot whales (*Globicephala melas*). *Sci. Rep.* 9, 1–10. <https://doi.org/10.1038/s41598-019-43825-z>.
- Burger, J., 1993. Metals in avian feathers: bioindicators of environmental pollution. *Rev. Environ. Toxicol.*
- Braune, B.M., Gaskin, D.E., 1987. Mercury Levels in Bonaparte's Gulls (*Larus philadelphia*) During Autumn Molt in the Quoddy Region, New Brunswick, Canada. *Arch. Environ. Contam. Toxicol.* 16, 539–549.
- Carlos, C.J., Voisin, J.-F., 2008. Identifying giant petrels, *Macronectes giganteus* and *M. halli*, in the field and in the hand. *Seabird* 21, 1–15.
- Cid-Barrio, L., Bouzas-Ramos, D., Salinas-Castillo, A., Ogra, Y., Encinar, J.R., Costa-Fernández, J.M., 2020. Quantitative assessment of cellular uptake and differential toxic effects of HgSe nanoparticles in human cells. *J. Anal. At. Spectrom.* 35, 1979–1988. <https://doi.org/10.1039/d0ja00162g>.
- Cipro, C.V.Z., Chérel, Y., Caurant, F., Miramand, P., Méndez-Fernandez, P., Bustamante, P., 2014. Trace elements in tissues of white-chinned petrels (*Procellaria aequinoctialis*) from Kerguelen waters, Southern Indian Ocean. *Polar Biol.* 37, 763–771. <https://doi.org/10.1007/s00300-014-1476-z>.
- Cuvin-Aralar, M.L.A., Furness, R.W., 1991. Mercury and selenium interaction: a review. *Ecotoxicol. Environ. Saf.* 21, 348–364. [https://doi.org/10.1016/0147-6513\(91\)90074-Y](https://doi.org/10.1016/0147-6513(91)90074-Y).
- Davis, W.C., Christopher, S.J., Pugh, R.S., Donard, O.F.X., Krupp, E.A., Point, D., Horvat, M., Gibicar, D., Kljakovic-Gaspic, Z., Porter, B.J., Schantz, M.M., 2007. Certification of methylmercury content in two fresh-frozen reference materials: SRM 1947 Lake Michigan fish tissue and SRM 1974b organics in mussel tissue (*Mytilus edulis*). *Anal. Bioanal. Chem.* 387, 2335–2341. <https://doi.org/10.1007/s00216-006-1106-x>.
- Davis, W.C., Long, S.E., 2011. Measurements of methylmercury, ethylmercury, and inorganic mercury species in a whole blood standard reference material: SRM 955c—toxic elements in caprine blood. *J. Anal. At. Spectrom.* 26, 431–435. <https://doi.org/10.1039/c0ja00175a>.
- Dehn, L.A., Sheffield, G.G., Follmann, E.H., Duffy, L.K., Thomas, D.L., Bratton, G.R., Taylor, R.J., O'Hara, T.M., 2005. Trace elements in tissues of phocid seals harvested in the Alaskan and Canadian Arctic: influence of age and feeding ecology. *Can. J. Zool.* 83, 726–746. <https://doi.org/10.1139/z05-053>.
- Du, B., Feng, X., Li, P., Yin, R., Yu, B., Sonke, J.E., Guinot, B., Anderson, C.W.N., Maurice, L., 2018. Use of mercury isotopes to quantify mercury exposure sources in Inland populations, China. *Environ. Sci. Technol.* 52, 5407–5416. <https://doi.org/10.1021/acs.est.7b05638>.
- Feng, C., Pedrero, Z., Gentès, S., Barre, J., Renedo, M., Tessier, E., Beral, S., Maury-Brachet, R., Mesmer-Dudons, N., Baudrimont, M., Legeay, A., Maurice, L., Gonzalez, P., Amouroux, D., 2015. Specific pathways of dietary methylmercury and inorganic mercury determined by mercury speciation and isotopic composition in Zebrafish (*Danio rerio*). *Environ. Sci. Technol.* 49, 12984–12993. <https://doi.org/10.1021/acs.est.5b03587>.
- Fitzgerald, W.F., Engstrom, D.R., Mason, R.P., Nater, E.A., 1998. The case for atmospheric mercury contamination in remote areas. *Environ. Sci. Technol.* 32, 1–7. <https://doi.org/10.1021/es970284w>.
- Fitzgerald, W.F., Lamborg, C.H., Hammerschmidt, C.R., 2007. Marine biogeochemical cycling of mercury. *Chem. Rev.* 107, 641–662. <https://doi.org/10.1021/cr050353m>.
- Foote, C.G., Daunt, F., González-Solís, J., Nasir, L., Phillips, R.A., Monaghan, P., 2011. Individual state and survival prospects: age, sex, and telomere length in a long-lived seabird. *Behav. Ecol.* 22, 156–161. <https://doi.org/10.1093/beheco/arq178>.
- Gajdoschova, Z., Lawan, M.M., Urgast, D.S., Raab, A., Scheckel, K.G., Lombi, E., Kopittke, P.M., Loeschner, K., Larsen, E.H., Woods, G., Brownlow, A., Read, F.L., Feldmann, J., Krupp, E.M., 2016. In vivo formation of natural HgSe nanoparticles in the liver and brain of pilot whales. *Sci. Rep.* 6, 1–11. <https://doi.org/10.1038/srep34361>.
- Kaercher, L.E., Goldschmidt, F., Paniz, J.N.G., De Moraes Flores, É.M., Dressler, V.L., 2005. Determination of inorganic and total mercury by vapor generation atomic absorption spectrometry using different temperatures of the measurement cell. *Spectrochim. Acta - Part B At. Spectrosc.* 60, 705–710. <https://doi.org/10.1016/j.sab.2005.03.006>.
- Kaschak, E., Knopf, B., Petersen, J.H., Bings, N.H., König, H., 2013. Biotic methylation of mercury by intestinal and sulfate-reducing bacteria and their potential role in mercury accumulation in the tissue of the soil-living *Eisenia foetida*. *Soil Biol. Biochem.* 69, 1–10. <https://doi.org/10.1016/j.soilbio.2013.11.004>.
- Khan, M.A.K., Wang, F., 2010. Chemical demethylation of methylmercury by selenoamino acids. *Chem. Res. Toxicol.* 23, 1202–1206. <https://doi.org/10.1021/tx100080s>.
- Kim, E.Y., Murakami, T., Saeki, K., Tatsukawa, R., 1996. Environmental contamination and toxicology mercury levels and its chemical form in tissues and organs of seabirds. *Arch. Environ. Contam. Toxicol.* 30, 259–266. <https://doi.org/10.1007/BF00215806>.
- Krupp, E.M., Mestrot, A., Wielgus, J., Meharg, A.A., Feldmann, J., 2009. The molecular form of mercury in biota: identification of novel mercury peptide complexes in plants. *Chem. Commun.* 28, 4257–4259. <https://doi.org/10.1039/b823121d>.
- Kwon, S.Y., Blum, J.D., Chirby, M.A., Chesney, E.J., 2013. Application of mercury isotopes for tracing trophic transfer and internal distribution of mercury in marine fish feeding experiments. *Environ. Toxicol. Chem.* 32, 2322–2330. <https://doi.org/10.1002/etc.2313>.
- Le Croizier, G., Lorrain, A., Sonke, J.E., Jaquemet, S., Schaal, G., Renedo, M., Besnard, L., Chérel, Y., Point, D., 2020. Mercury isotopes as tracers of energy and metabolism in two sympatric shark species. *Environ. Pollut.* 265, 114931. <https://doi.org/10.1016/j.envpoll.2020.114931>.
- Li, M., Juang, C.A., Ewald, J.D., Yin, R., Mikkelsen, B., Krabbenhoft, D.P., Balcom, P.H., Dassuncao, C., Sunderland, E.M., 2020. Selenium and stable mercury isotopes provide new insights into mercury toxicokinetics in pilot whales. *Sci. Total Environ.* 710, 136325. <https://doi.org/10.1016/j.scitotenv.2019.136325>.
- Ma, L., Evans, R.D., Wang, W., Georg, R.B., 2018. In vivo fractionation of mercury isotopes in tissues of a mammalian carnivore (Neovivipar). *Sci. Total Environ.* 627, 1228–1233. <https://doi.org/10.1016/j.scitotenv.2018.01.296>.
- Manceau, A., Azemard, S., Hédouin, L., Vassileva, E., Lecchini, D., Fauvelot, C., Swarzenski, P.W., Glatzel, P., Bustamante, P., Metian, M., 2021a. Chemical forms of mercury in blue marlin billfish: implications for human exposure. *Environ. Sci. Technol. Lett.* 8, 405–411. <https://doi.org/10.1021/acs.estlett.1c00217>.
- Manceau, A., Brossier, R., Janssen, S.E., Rosera, T.J., Krabbenhoft, D.P., Chérel, Y., Bustamante, P., Poulin, B.A., 2021b. Mercury isotope fractionation by internal demethylation and biomineralization reactions in seabirds: implications for environmental mercury science. *Environ. Sci. Technol.* 55, 13942–13952. <https://doi.org/10.1021/acs.est.1c04388>.
- Manceau, A., Gaillot, A.C., Glatzel, P., Chérel, Y., Bustamante, P., 2021c. In vivo formation of HgSe nanoparticles and Hg-tetraselenolate complex from methylmercury in seabirds – implications for the Hg-Se antagonism. *Environ. Sci. Technol.* 55, 1515–1526. <https://doi.org/10.1021/acs.est.0c06269>.
- Masbou, J., Sonke, J.E., Amouroux, D., Guillou, G., Becker, P.R., Point, D., 2018. Hg-stable isotope variations in marine top predators of the western Arctic ocean. *ACS Earth Sp. Chem.* 2, 479–490. <https://doi.org/10.1021/acsearthspacechem.8b00017>.
- Mason, R.P., 2013. The methylation of metals and metalloids in aquatic systems. In: *Methylation – From DNA, RNA and Histones to Diseases and Treatment*. Intech, pp. 271–301.
- Mason, R.P., Reinfelder, J.R., Morel, F.M.M., 1995. Bioaccumulation of mercury and methylmercury. *Water Air Soil Pollut.* 80, 915–921. <https://doi.org/10.1007/BF01189744>.

- Meredith, A., Johnson-Delaney, C., 2010. BSAVA Manual of Exotic Pets. 5th Editio. ed. British Small Animal Veterinary Association, Quedgeley.
- Mills, W.F., Bustamante, P., McGill, R.A.R., Anderson, O.R.J., Bearhop, S., Cherel, Y., Votier, S.C., Phillips, R.A., 2020. Mercury exposure in an endangered seabird: Long-term changes and relationships with trophic ecology and breeding success: Mercury exposure in albatrosses. *Proc. R. Soc. B Biol. Sci.* 287, 20202683. <https://doi.org/10.1098/rspb.2020.2683>.
- Palmer, J.H., Parkin, G., 2015. Protolytic cleavage of Hg—C bonds induced by 1-methyl-1,3-dihydro-2H-benzimidazole-2-selone: synthesis and structural characterization of mercury complexes. *J. Am. Chem. Soc.* 137, 4503–4516. <https://doi.org/10.1021/jacs.5b00840>.
- Palmisano, F., Cardellicchio, N., Zamboni, P.G., 1995. Speciation of mercury in dolphin liver: a two-stage mechanism for the demethylation accumulation process and role of selenium. *Mar. Environ. Res.* 40, 109–121. [https://doi.org/10.1016/0141-1136\(94\)00142-C](https://doi.org/10.1016/0141-1136(94)00142-C).
- Pedrero, Z., Donard, O.F.X., Amouroux, D., 2016. Pushing back the frontiers of mercury speciation using a combination of biomolecular and isotopic signatures: challenge and perspectives. *Anal. Bioanal. Chem.* 408, 2641–2648. <https://doi.org/10.1007/s00216-015-9243-8>.
- Pedrero, Z., Mounicou, S., Monperrus, M., Amouroux, D., 2011. Investigation of Hg species binding biomolecules in dolphin liver combining GC and LC-ICP-MS with isotopic tracers. *J. Anal. At. Spectrom.* 26, 187–194. <https://doi.org/10.1039/c0ja00154f>.
- Pedrero, Z., Ouerdane, L., Mounicou, S., Lobinski, R., Monperrus, M., Amouroux, D., 2012. Identification of mercury and other metals complexes with metallothioneins in dolphin liver by hydrophilic interaction liquid chromatography with the parallel detection by ICP MS and electrospray hybrid linear/orbital trap MS/MS. *Metallomics* 4, 473–479. <https://doi.org/10.1039/c2mt00006g>.
- Pedrero Zayas, Z., Ouerdane, L., Mounicou, S., Lobinski, R., Monperrus, M., Amouroux, D., 2014. Hemoglobin as a major binding protein for methylmercury in white-sided dolphin liver. *Anal. Bioanal. Chem.* 406, 1121–1129. <https://doi.org/10.1007/s00216-013-7274-6>.
- Perrot, V., Epov, V.N., Valentina, M.V.P., Grebenshchikova, I., Zouiten, C., Sonke, J.E., Husted, S., Donard, O.F.X., Amouroux, D., 2010. Tracing sources and bioaccumulation of mercury in fish of Lake Baikal – Angara River using Hg isotopic composition. *Environ. Sci. Technol.* 44, 8030–8037. <https://doi.org/10.1021/es101898e>.
- Perrot, V., Masbou, J., Pastukhov, M.V., Epov, V.N., Point, D., Bérail, S., Becker, P.R., Sonke, J.E., Amouroux, D., 2016. Natural Hg isotopic composition of different Hg compounds in mammal tissues as a proxy for in vivo breakdown of toxic methylmercury. *Metallomics* 8, 170–178. <https://doi.org/10.1039/C5MT00286A>.
- Poulin, B.A., Janssen, S.E., Rosera, T.J., Krabbenhoft, D.P., Eagles-smith, C.A., Ackerman, J.T., Stewart, A.R., Kim, E., Kim, J., Manceau, A., 2021. Isotope fractionation from in vivo methylmercury detoxification in waterbirds. *ACS Earth Sp. Chem.* 5, 990–997. <https://doi.org/10.1021/acsearthspacechem.1c00051>.
- Renedo, M., Amouroux, D., Duval, B., Carravieri, A., Tessier, E., Barre, J., Bérail, S., Pedrero, Z., Cherel, Y., Bustamante, P., 2018a. Seabird tissues as efficient biomonitoring tools for Hg isotopic investigations: implications of using blood and feathers from chicks and adults. *Environ. Sci. Technol.* 52, 4227–4234. <https://doi.org/10.1021/acs.est.8b00422>.
- Renedo, M., Amouroux, D., Pedrero, Z., Bustamante, P., Cherel, Y., 2018b. Identification of sources and bioaccumulation pathways of MeHg in subantarctic penguins: a stable isotopic investigation. *Sci. Rep.* 8, 1–10. <https://doi.org/10.1038/s41598-018-27079-9>.
- Renedo, M., Bustamante, P., Cherel, Y., Pedrero, Z., Tessier, E., Amouroux, D., 2020. A “seabird-eye” on mercury stable isotopes and cycling in the Southern Ocean. *Sci. Total Environ.* 742, 742. <https://doi.org/10.1016/j.scitotenv.2020.140499>.
- Renedo, M., Bustamante, P., Tessier, E., Pedrero, Z., Cherel, Y., Amouroux, D., 2017. Assessment of mercury speciation in feathers using species-specific isotope dilution analysis. *Talanta* 174, 100–110. <https://doi.org/10.1016/j.talanta.2017.05.081>.
- Renedo, M., Pedrero, Z., Amouroux, D., Cherel, Y., Bustamante, P., 2021. Mercury isotopes of key tissues document mercury metabolic processes in seabirds. *Chemosphere* 263, 127777. <https://doi.org/10.1016/j.chemosphere.2020.127777>.
- Rheindt, F.E., Austin, J.J., 2005. Major analytical and conceptual shortcomings in a recent taxonomic revision of the Procellariiformes – a reply to Penhallurick and Wink (2004). *Emu* 105, 181–186. <https://doi.org/10.1071/MU04039>.
- Rodríguez-González, P., Epov, V.N., Bridou, R., Tessier, E., Guyoneaud, R., Monperrus, M., Amouroux, D., 2009. Species-specific stable isotope fractionation of mercury during Hg(II) methylation by an anaerobic bacteria (*Desulfobulbus propionicus*) under dark conditions. *Environ. Sci. Technol.* 43, 9183–9188. <https://doi.org/10.1021/es902206j>.
- Salomon, M., Voisin, J.F., 2010. Ecogeographical variation in the southern giant petrel (*Macronectes giganteus*). *Can. J. Zool.* 88, 195–203. <https://doi.org/10.1139/Z09-134>.
- Seewagen, C.L., Cristol, D.A., Gerson, A.R., 2016. Mobilization of mercury from lean tissues during simulated migratory fasting in a model songbird. *Sci. Rep.* 6, 6–10. <https://doi.org/10.1038/srep25762>.
- Sherman, L.S., Blum, J.D., Basu, N., Rajae, M., Evers, D.C., Buck, D.G., Petrik, J., DiGangi, J., 2015. Assessment of mercury exposure among small-scale gold miners using mercury stable isotopes. *Environ. Res.* 137, 226–234. <https://doi.org/10.1016/j.envres.2014.12.021>.
- Sherman, L.S., Blum, J.D., Franzblau, A., Basu, N., 2013. New insight into biomarkers of human mercury exposure using naturally occurring mercury stable isotopes. *Environ. Sci. Technol.* 47, 3403–3409. <https://doi.org/10.1021/es305250z>.
- Stewart, F.M., Phillips, R.A., Bartle, A.J., Craig, J., Shooter, D., 1999. Influence of phylogeny, diet, moult schedule and sex on heavy metal concentrations in New Zealand Procellariiformes. *Mar. Ecol. Prog. Ser.* 178, 295–305. <https://doi.org/10.3354/meps178295>.
- Thiers, L., Delord, K., Barbraud, C., Phillips, R.A., Pinaud, D., Weimerskirch, H., 2014. Foraging zones of the two sibling species of giant petrels in the Indian Ocean throughout the annual cycle: implication for their conservation. *Mar. Ecol. Prog. Ser.* 499, 233–248. <https://doi.org/10.3354/meps10620>.
- Thompson, D.R., Furness, R.W., 1989. The chemical form of mercury stored in South Atlantic seabirds. *Environ. Pollut.* 60, 305–317. [https://doi.org/10.1016/0269-7491\(89\)90111-5](https://doi.org/10.1016/0269-7491(89)90111-5).
- Trümpler, S., Lohmann, W., Meermann, B., Buscher, W., Sperling, M., Karst, U., 2009. Interaction of thimerosal with proteins – ethylmercury adduct formation of human serum albumin and β -lactoglobulin A. *Metallomics* 1, 87–91. <https://doi.org/10.1039/b815978e>.
- Wone, B.W.M., Kinchen, J.M., Kaup, E.R., Wone, B., 2018. A procession of metabolic alterations accompanying muscle senescence in *Manduca sexta*. *Sci. Rep.* 8, 1–13. <https://doi.org/10.1038/s41598-018-19630-5>.
- Yamashita, M., Yamashita, Y., Suzuki, T., Kani, Y., Mizusawa, N., Imamura, S., Takemoto, K., Hara, T., Hossain, M.A., Yabu, T., Touhata, K., 2013. Selenoneine, a novel selenium-containing compound, mediates detoxification mechanisms against methylmercury accumulation and toxicity in zebrafish embryo. *Mar. Biotechnol.* 15, 559–570. <https://doi.org/10.1007/s10126-013-9508-1>.